

# Correlation of the Structure, Properties, and Antimicrobial Activity of a Soluble Thiolated Chitosan Derivative

Bing Han,<sup>1</sup> Yan Wei,<sup>2</sup> Xiaolong Jia,<sup>3</sup> Juan Xu,<sup>3</sup> Gang Li<sup>3</sup>

<sup>1</sup>Department of Orthodontics, Peking University School and Hospital of Stomatology, Beijing 100081, People's Republic of China

<sup>2</sup>Department of Geriatric Dentistry, Peking University School and Hospital of Stomatology, Beijing 100081, People's Republic of China

<sup>3</sup>State Key Laboratory of Organic-Inorganic Composites, Beijing University of Chemical Technology, Beijing 100029, People's Republic of China

Received 16 June 2011; accepted 27 November 2011

DOI 10.1002/app.36548

Published online 6 March 2012 in Wiley Online Library (wileyonlinelibrary.com).

**ABSTRACT:** A thiolated chitosan (CS) derivative was synthesized by the introduction of thioglycolic acid to CS via amide-bond formation mediated by carbodiimide. The chemical structure of the CS derivative was confirmed by Fourier transform infrared spectroscopy and <sup>1</sup>H-NMR spectroscopy. The solubility test showed that the thiolated CS derivative was water-soluble. The X-ray pattern of the CS derivative showed an obvious disappearance or shift of crystalline peaks compared to that of CS. Thermogravimetric

analysis indicated that the degradation peak temperature of the thiolated CS derivative was much higher than that of CS and implied an improved thermal stability at higher temperatures. Moreover, the antimicrobial activity of the thiolated CS derivative was comparable to that of CS. © 2012 Wiley Periodicals, Inc. *J Appl Polym Sci* 125: E143–E148, 2012

**Key words:** biological applications of polymers; biomaterials; biopolymers

## INTRODUCTION

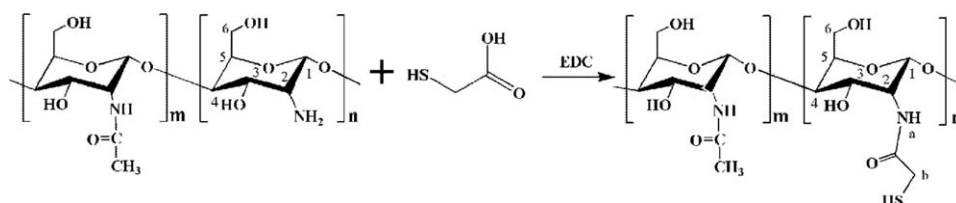
The biopolymer chitosan (CS) is currently a focus of scientific and economic interest because of its unique properties, including its biocompatibility, biodegradability, nontoxicity, and excellent film-forming ability.<sup>1–4</sup> It has been used in tissue engineering, drug-delivery systems, wound healing, and antimicrobial agents.<sup>5–7</sup> However, the applications of CS have been severely limited because of its insolubility in neutral aqueous solutions and organic solvents; this insolubility results from its compact crystalline structure and deacetylation. To improve the solubility and widen the applications of CS, various CS derivatives have been prepared by chemical modifications,<sup>8–11</sup> which keep the fundamental skeleton and the original physicochemical and biochemical properties of CS and bring new specialties ascribed to the characteristics of the introduced groups.<sup>12</sup> Particularly, modifications of the  $-\text{CH}_2\text{OH}$  and  $-\text{NH}_2$  groups on the CS chain dedicated to higher reactive activity and better ductility have been very favorable.<sup>13</sup>

The thiol group ( $-\text{SH}$ ) is a chemical analogue of the hydroxyl group ( $-\text{OH}$ ) and, thus, indicates the

great potential of enhancing the properties of CS. CS derivatives can be obtained through the reaction of the thiol group ( $-\text{SH}$ ) and the primary amine ( $-\text{NH}_2$ ) of CS. At present, four types of thiolated CS derivatives have been generated; conjugates include CS–cysteine, CS–4-thiobutylamidine, CS–thioethylamidine, and CS–thioglycolic acid (TGA).<sup>14–17</sup> Particularly, the CS–thioglycolic conjugate has exhibited promising use for tissue engineering because of its water solubility, controllable biodegradation, and *in situ* gelling.<sup>17,18</sup> Meanwhile, the mucoadhesive properties, permeation-enhancing effects, and cohesive properties have been greatly enhanced by the formation of a disulfide bond ( $\text{R}-\text{S}-\text{S}-\text{R}'$ ) with cysteine residues in proteins;<sup>2,19–21</sup> these changes make it suitable for drug delivery in physical forms, such as gels, powder and films.<sup>22</sup> However, few studies have been reported on the interrelationship between the chemical structure, physical properties, and antibiosis of thiolated CS derivatives.

In this article, a thiolated CS derivative was synthesized by the covalent link conjugation of CS with TGA. The chemical structure and physical properties of the thiolated CS derivative were characterized by Fourier transform infrared (FTIR) spectroscopy, <sup>1</sup>H-NMR spectroscopy, solubility testing, X-ray diffraction (XRD), and thermogravimetric (TG) analysis. The antimicrobial activity of the CS and thiolated CS derivative were investigated by the plate count agar

Correspondence to: X. Jia (jiaxl@mail.buct.edu.cn) or G. Li (ligang@mail.buct.edu.cn).



Scheme 1 Synthesis procedure of the thiolated CS derivative.

method. Furthermore, the interrelationships of the structure, properties, and antibiosis of the thiolated CS derivative were analyzed.

## EXPERIMENTAL

### Synthesis of the CS derivative

The synthesis procedure of the thiolated CS derivative was carried out according to Scheme 1. First, 500 mg of CS (molecular weight =  $2.0 \times 10^4$  and deacetylation degree  $\approx 88.0\%$ , Yuhuan Ocean Biochemical Co., Ltd., Zhejiang, China) was hydrated in 4 mL of HCl (1M) at room temperature and dissolved in 46 mL of deionized water to obtain a solution of chitosan hydrochloride. Thereafter, 500 mg of TGA (Aldrich, reagent, Sigma, New York, USA) and 4 mL of 1-ethyl-3-(3-dimethylaminopropyl) carbon diimide hydrochloride (EDC; Sigma, New York, USA) were added to the solution of chitosan hydrochloride under stirring. The reaction mixture was incubated at pH 5 for 5 h at room temperature by agitation.

To eliminate unbound TGA and other reagents, the reaction mixture was dialyzed in a tube at  $10^\circ\text{C}$  five times. In detail, the mixture was dialyzed once against 5 mM HCl and then twice against a solution of 5 mM HCl and 1% NaCl; thereafter, the samples were dialyzed twice against 1 mM HCl (every time for 10 h). Finally, the samples were lyophilized and stored at  $4^\circ\text{C}$  for further use.

### Characterization of the CS derivative

#### FTIR spectra

The FTIR spectra of the CS and CS derivative were measured in the  $4000\text{--}500\text{-cm}^{-1}$  regions with a Nicolet 5700 instrument (Nicolet Instruments, Thermo Co., Cherry Hill, New Jersey, USA). The samples were prepared as KBr pellets and were scanned against a blank KBr pellet background in the wave-number range  $4000\text{--}500\text{ cm}^{-1}$  with a resolution of  $4.0\text{ cm}^{-1}$ .

#### $^1\text{H-NMR}$ spectra

The  $^1\text{H-NMR}$  spectra were obtained on a Bruker AV 600-MHz instrument (Bruker, Rheinstetten, Germany). The CS and CS derivative were dissolved in a mixed solvent of  $\text{CD}_3\text{COOD}$  and  $\text{D}_2\text{O}$ . The degree of

substitution (DS) of the CS derivative was calculated from the peak area at 2.1 ppm of the  $\text{CH}_2\text{b}$  proton against that at 1.9 ppm of the Amino Acetylation (NHAc) proton.<sup>23</sup>

#### Solubility test

The solubility values of the CS and thiolated CS derivative in distilled water and organic solvents were qualitatively evaluated according to an approach in the literature.<sup>24</sup> Five milligrams of CS or thiolated CS derivative was mixed with 1 mL of distilled water or organic solvent, stirred for 5 h at room temperature, and then filtered through filter paper. The increase in the filter-paper weight indicated that the CS derivative was insoluble.

#### XRD

The XRD patterns of the sheet samples were obtained on an X-ray diffractometer (D/Max2500VB2+/Pc, Rigaku Co., Tokyo, Japan) with an area detector operating at a 40-kV voltage and a 50-mA current with Cu  $\text{K}\alpha$  radiation ( $\lambda = 0.154\text{ nm}$ ). The scanning rate was  $1^\circ/\text{min}$ , and the scanning scope of  $2\theta$  was from  $5$  to  $50^\circ$  at room temperature.

#### TG analysis

TG analysis was carried out with a Q600 TG analysis/differential scanning calorimetry instrument (TA Instruments Co., New Castle, Delaware, USA) under a nitrogen atmosphere at a 40 mL/min purge rate. The samples were heated at a rate of  $10^\circ\text{C}/\text{min}$ . Samples of 10–12 mg were used.

#### Antimicrobial activity

The antibacterial activities of the CS and thiolated CS derivatives against *Escherichia coli* (*E. coli*, ATCC 25922, America Type Culture Collection, Manassas, VA) were determined by the plate count agar method. First, a nutrient agar slope consisting of 1.0 g of peptone, 0.5 g of NaCl, 0.3 g of beef extract, and 2 g of agar was prepared; the suspension was prepared by the transfer of sterile 0.9% saline to this slope. Then, 10-fold dilutions were carried out to obtain antibacterial testing solutions (concentration

= 600 cells/mL). To eliminate the effect of acetic acid (HAc) on the antimicrobial activity, an HAc solution was also prepared and used as a reference. The CS and CS derivative were, respectively, dissolved in a 0.3% v/v HAc solution to obtain 0.5 wt % solutions, and the solutions were microfiltered through a syringe filter. Finally, the solutions were added to the previous suspensions to produce mixtures with 150-ppm concentrations. The mixtures were shaken gently to disperse HAc, CS, and CS derivative throughout the agar plates. Afterward, 0.4 mL of each diluted bacteria solution was spread onto an agar plate. After incubation at 37°C for 24 h, the number of colonies was counted to measure the antibacterial activity. The survival percentage was calculated as follows:<sup>25</sup>

$$\text{Survival(\%)} = \frac{\text{Colonies of treated bacteria}}{\text{Colonies of controlled bacteria}} \times 100\%$$

## RESULTS AND DISCUSSION

### FTIR analysis

Figure 1 shows the FTIR spectra of the CS and thiolated CS derivative. The characteristic vibration peaks of CS were clearly observed. The broad peak at 3440  $\text{cm}^{-1}$  was assigned to  $-\text{OH}$  and  $-\text{NH}$  stretching vibrations, and the weak peak at 2920  $\text{cm}^{-1}$  was attributed to  $-\text{CH}$  stretching. The distinctive absorption peaks appearing at 1660, 1590, and 1380  $\text{cm}^{-1}$  were attributed to amide I,  $-\text{NH}_2$  bending, and amide III,<sup>26</sup> respectively. The peak at 1030  $\text{cm}^{-1}$  was due to  $\text{C}-\text{O}-\text{C}$  stretching and the saccharine structure.<sup>27</sup> In the spectra of the thiolated CS derivative, a distinct absorption peak at 1732  $\text{cm}^{-1}$  cor-

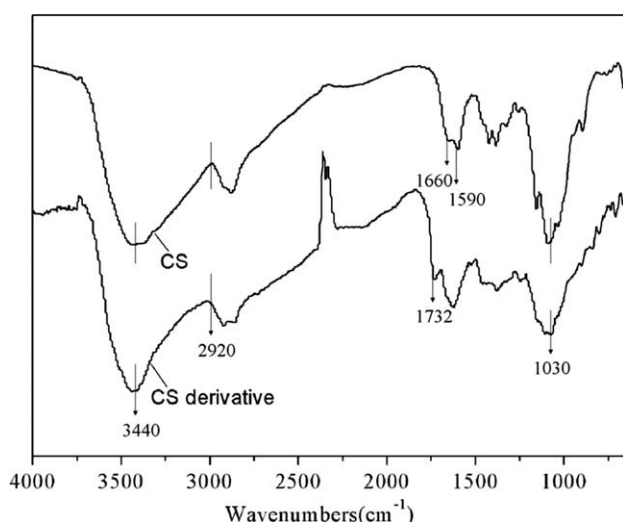


**Figure 1** FTIR spectra of the CS and thiolated CS derivative.

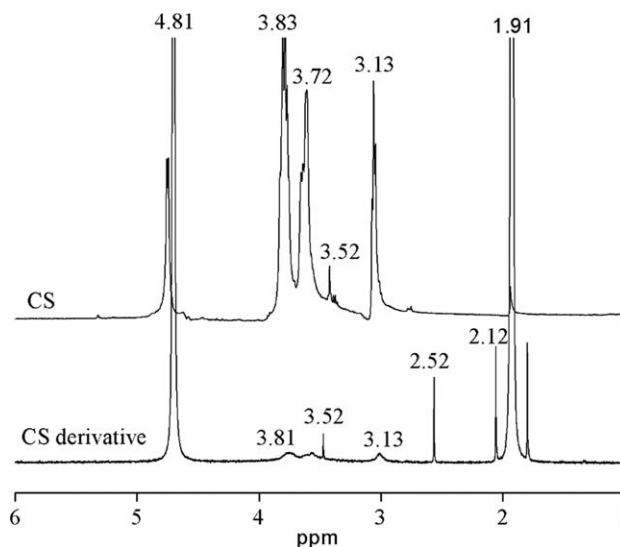


**Figure 2**  $^1\text{H-NMR}$  spectra of the CS and thiolated CS derivative.

responded to the carbonyl groups of TGA, and the decreased peak at 1590  $\text{cm}^{-1}$  was assigned to  $-\text{NH}$  bending and implied that the carbonyl groups of TGA were successfully introduced into the chemical structure of the CS derivative. Additionally, the special shape of the peak at 2350  $\text{cm}^{-1}$  was due to  $\text{CO}_2$  in the air; this was also found by Ma et al.<sup>28</sup>

### $^1\text{H-NMR}$ spectra

The  $^1\text{H-NMR}$  spectra of the CS and thiolated CS derivative are shown in Figure 2. The small peak at 1.9 ppm was attributed to the  $-\text{CH}_3$  of the *N*-acetyl glucosamine (GlcN) residue. The peak at 3.10 ppm existed because of the  $\text{H}_2$  of GlcN and *N*-alkylated GlcN,<sup>29</sup> and the peaks from 3.5–3.8 ppm were assigned to  $\text{H}_3$ ,  $\text{H}_4$ ,  $\text{H}_5$ , and  $\text{H}_6$  of the methane protons of GlcN and *N*-alkylated GlcN. The intense peak at 4.8 ppm was related to the  $\text{H}_1$  of GlcN and *N*-alkylated GlcN. In the spectra of the thiolated CS derivative, there still appeared some peaks similar to those of CS. However, a new peak at 2.1 ppm was observed, which corresponded to  $\text{H}_b$  and resulted from the existence of the  $\text{CH}_2$  groups, and the peak at 2.5 ppm was assigned to  $\text{H}_a$ , which indicated the generation of  $-\text{NH}$  groups. In general, the DS was directly related to the solubility and antimicrobial activity of the CS derivative, and DS could be changed by different ratios of  $-\text{NH}_2$  and  $-\text{SH}$  on CS and different reaction temperatures and reaction times. Therefore, DS was calculated from the peak area at the chemical shift of the  $-\text{CH}_2$  proton against that of  $\text{NHAc}$  proton.<sup>23</sup> The ratio of peak area at  $\delta = 2.1$  and 1.9 ppm was about 0.27; thus, the DS of the CS derivative was 0.27; this was favorable for the swelling and dissolution of the derivative in water.

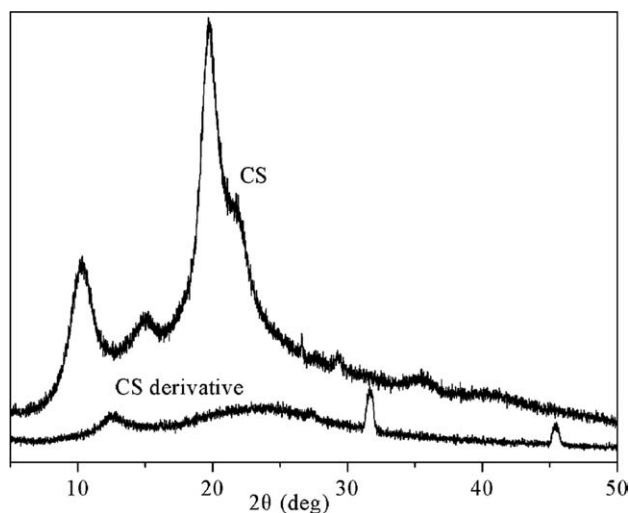


**Figure 3** XRD patterns of the CS and thiolated CS derivative.

### XRD

The effects of intermolecular and extramolecular interactions on the crystallization structure of the CS and thiolated CS derivative were examined with XRD. Figure 3 gives the XRD patterns of the CS and thiolated CS derivative. Three reflections located at  $2\theta = 10.3$ ,  $15.9$ , and  $20.1^\circ$  were present in the XRD pattern of CS; this was in agreement with previous reports.<sup>30,31</sup> The strong reflection fall at  $2\theta = 20.1^\circ$ , assigned to crystal form II, and the peak at  $2\theta = 10.3^\circ$ , corresponding to crystal form I, indicated the high degree crystallinity of CS, which may have been due to the hydrogen bonding of intermoleculars and extramoleculars, as discussed in a previous report.<sup>32</sup> The XRD pattern of the thiolated CS derivative was significantly different from that of CS. The sharp peaks at  $2\theta = 10.3$  and  $20.1^\circ$  disappeared, whereas a broad reflection at about  $2\theta = 22.1^\circ$  and a weak reflection at about  $2\theta = 11.8^\circ$  were present. This disappearance or shift of the crystalline peaks indicated the disruption of the ordered structure of the CS by chemical modification, and the thiolated CS derivative became amorphous.

**TABLE I**  
Solubility of the CS and Thiolated CS Derivative

Solvent	Solubility	
	CS	CS derivative
Distilled water	× <sup>a</sup>	√ <sup>b</sup>
Chloroform	× <sup>a</sup>	× <sup>a</sup>
<i>N,N'</i> -Dimethylformamide	× <sup>a</sup>	× <sup>a</sup>

<sup>a</sup> Insoluble.

<sup>b</sup> Soluble.

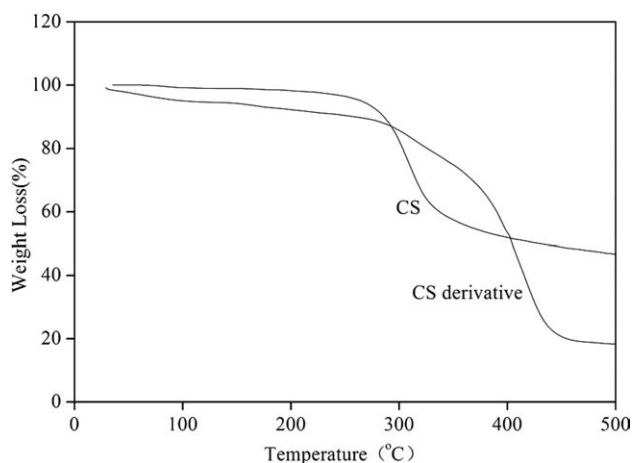


**Figure 4** TG curves of the CS and thiolated CS derivative.

### Solubility evaluation

The solubility of the CS and thiolated CS derivative in distilled water and organic solvents are shown in Table I. It was obvious that both the CS and CS derivative could not dissolve in chloroform or *N,N'*-dimethylformamide. CS was insoluble in distilled water, whereas the CS derivative showed favorable solubility in distilled water; this was attributed to the amorphous structure resulting from the decreased forming ability of hydrogen bonds due to the generation of thiol substitution.

### TG analysis

Figures 4 and 5 reveal the TG and thiolated derivative thermogravimetric (DTG) curves of the CS and CS derivative. As shown by the TG curves, two stages occurred during the degradation of CS. The first stage began at about  $100^\circ\text{C}$  due to the loss of residual or physically adsorbed water, and the second

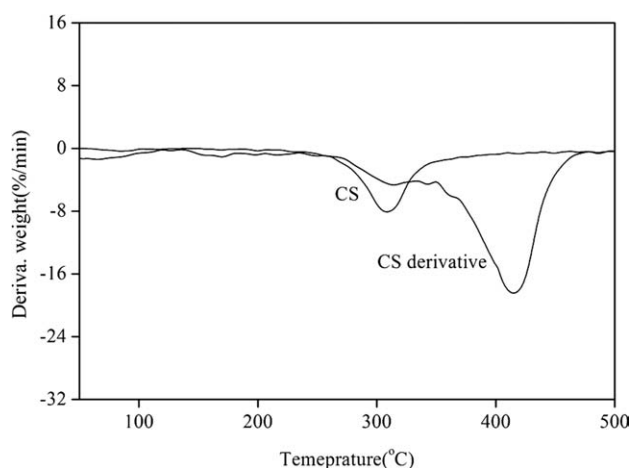


**Figure 5** DTG curves of the CS and thiolated CS derivative.

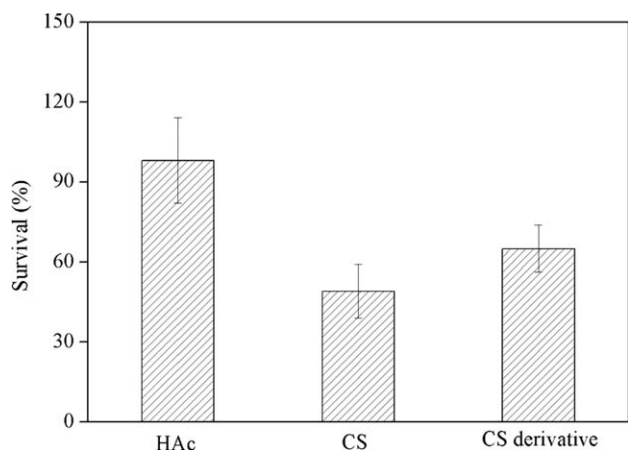


**Figure 6** Antibacterial activity of the HAc, CS, and thiolated CS derivative against *E. coli*.

stage showed a rapid weight loss at about 260°C. The DTG curve of the CS derivative also showed two major degradation steps assigned by CS and the grafted groups individually. In contrast with the peak of CS at 308°C, a flat peak at 309°C and a sharp peak at 420°C were present in the CS derivative; these clearly revealed that the degradation peak temperature of the CS derivative was higher than that of CS. Additionally, the sharp peak showed that the CS derivative degraded very fast in the temperature range close to 420°C; this resulted from a series of complex chemical changes in the process, including the sugar-ring dehydration, degradation, molecular chain acetaminophen, and *N*-deacetylation of the cracking unit,<sup>33</sup> and the disruption of the ordered structure of CS by the introduction of the —SH.

#### Antimicrobial activity of the CS and CS derivative

The antimicrobial activities of the HAc, CS, and CS derivative against *E. coli* are shown in Figure 6. At a 150-ppm concentrations of HAc, there was a slight effect on the growth of *E. coli*, which was due to the possible balance between the promotional and inhibitory effects of HAc at this level of concentration. The result was in agreement with the published report by Xiao et al.<sup>34</sup> However, the CS and thiolated CS derivative showed the effective suppression of *E. coli* bacteria. CS adsorbed the electronegative substance in the cell attributed to the electropositive from the amino groups at the C<sub>2</sub> position and could prevent the transportation of essential nutrients entering cell through the formation of a polymer membrane.<sup>35,36</sup> Therefore, the destruction of the physiological activities of the bacteria resulted in a severe leakage of cell constituents and eventually to the death of the cell. Compared to that of CS, the antimicrobial activity of the CS derivative was a lit-

tle weaker; this implied that a CS derivative with a higher DS may possess a lower antimicrobial activity, similar to the previous report.<sup>28</sup> However, the CS derivative still exhibited valid suppression of *E. coli* bacteria; this was due to the reduction of the concentration of amino groups at the C<sub>2</sub> position of the CS derivative, which resulted from the reaction of the thiol groups and —NH<sub>2</sub> groups.

#### CONCLUSIONS

A thiolated CS derivative was successfully prepared by the introduction of thiol groups to CS, and the chemical structure was verified by FTIR and <sup>1</sup>H-NMR spectroscopy. The CS derivative was amorphous and water-soluble because of the disruption of the ordered structure of CS by chemical modification, and the degradation peak temperature of the CS derivative was increased. The antimicrobial activity of the CS derivative remained almost invariable, although the consumption of amino groups occurred during the reaction of the thiol groups and primary amine. Its favorable water solubility and excellent antimicrobial activity suggested that the CS derivative possesses great application potential for tissue engineering and drug delivery.

#### References

1. Wang, J. T.; Jin, X. X.; Chang, D. F. *Carbohydr Polym* 2009, 78, 175.
2. Bernkop-Schnürch, A.; Hornof, M.; Gugli, D. *Eur J Pharm Biopharm* 2004, 57, 9.
3. Tang, F.; Zhang, L. F.; Zhu, J.; Cheng, Z. P.; Zhu, X. L. *Ind Eng Chem Res* 2009, 48, 6216.
4. Zhong, Z. M.; Xing, R. G.; Liu, S.; Wang, L.; Cai, S. G.; Li, P. C. *Carbohydr Res* 2008, 343, 566.
5. Wang, Y. C.; Lin, M. C.; Wang, D. M.; Hsieh, H. J. *Biomaterials* 2003, 24, 1047.
6. Saboktakin, M. R.; Tabatabaee, R. M.; Maharramov, A.; Ramazanov, M. A. *Carbohydr Polym* 2010, 82, 466.
7. Minagawa, T.; Okamura, Y.; Shigemasa, Y.; Minami, S.; Okamoto, Y. *Carbohydr Polym* 2007, 67, 640.
8. Zhong, Z. M.; Li, P. C.; Xing, R. G.; Liu, S. *Int J Biol Macromol* 2009, 45, 163.
9. Heras, A.; Rodríguez, N. M.; Ramos, V. M.; Agulló, E. *Carbohydr Polym* 2001, 44, 1.
10. Lin, H. Y.; Chou, C. C. *Food Res Int* 2004, 37, 883.
11. Sajomsang, W.; Gonil, P.; Saesoo, S. *Eur Polym J* 2009, 45, 2319.
12. Gao, X. Y.; Zhou, Y. S.; Ma, G. P.; Shi, S. Q.; Yang, D. Z.; Lu, F. M.; Nie, J. *Carbohydr Polym* 2010, 79, 507.
13. Alves, N. M.; Mano, J. F. *Int J Biol Macromol* 2008, 43, 401.
14. Schmitz, T.; Grabovac, V.; Palmberger, T. F.; Hoffer, M. H.; Bernkop-Schnürch, A. *Int J Pharm* 2008, 347, 79.
15. Gugli, D.; Langoth, N.; Hoffer, M. H.; Wirth, M.; Bernkop-Schnürch, A. *Int J Pharm* 2004, 278, 353.
16. Kafedjiski, K.; Hoffer, M.; Werle, M.; Bernkop-Schnürch, A. *Biomaterials* 2006, 27, 127.
17. Kast, C. E.; Frick, W.; Losert, U.; Bernkop-Schnürch, A. *Int J Pharm* 2003, 256, 183.

18. Saboktakin, M. R.; Tabatabaie, R. M.; Maharramov, A.; Ramazanov, M. A. *Int J Biol Macromol* 2011, 48, 403.
19. Munro, N. H.; Hanton, L. R.; Moratti, S. C.; Robinson, B. H. *Carbohydr Polym* 2009, 78, 137.
20. Bernkop-Schnürch, A.; Kast, C. E.; Guggi, D. *J Controlled Release* 2003, 93, 95.
21. Constantine, C. A.; Gattás-Asfura, K. M.; Mello, S. V.; Crespo, G.; Rastogi, V.; Cheng, T. C.; DeFrank, J. J.; Leblanc, R. M. *J Phys Chem B* 2003, 107, 13762.
22. Cathell, M. D.; Szewczyk, J. C.; Bui, F. A.; Weber, C. A.; Wolever, J. D.; Kang, J.; Schauer, C. L. *Biomacromolecules* 2008, 9, 289.
23. Sashiwa, H.; Yamamori, N.; Ichinose, Y.; Sunamoto, J.; Aiba, S. *Biomacromolecules* 2003, 4, 1250.
24. Ying, G. Q.; Xiong, W. Y.; Wang, H.; Sun, Y.; Liu, H. Z. *Carbohydr Polym* 2011, 83, 1787.
25. Lu, Z. S.; Li, C. M.; Bao, H. F.; Qiao, Y.; Hoh, Y. H.; Yang, X. *Langmuir* 2008, 24, 5445.
26. Zang, C.; Ping, Q. N.; Zhang, H. J.; Shen, J. *Eur Polym J* 2003, 39, 1629.
27. Peniche, C.; Arguelles-Monal, W.; Davidenko, N.; Sastre, R.; Gallardo, A.; SanRoman, J. *Biomaterials* 1999, 20, 1869.
28. Ma, G. P.; Zhang, X. D.; Han, J.; Song, G. Q.; Nie, J. *Int J Biol Macromol* 2009, 45, 499.
29. Wu, Y.; Zheng, Y. L.; Wang, C. C.; Hu, J. H.; Fu, S. K. *Carbohydr Polym* 2005, 59, 165.
30. Zhang, Y. Q.; Xue, C. H.; Xue, Y.; Gao, R. C.; Zhang, X. L. *Carbohydr Res* 2005, 340, 1914.
31. Wu, H.; Zhang, J.; Xiao, B.; Zan, X. L.; Gao, J.; Wan, Y. *Carbohydr Polym* 2011, 83, 824.
32. Samuels, R. J. *J Polym Sci Polym Phys Ed* 1981, 19, 1081.
33. Peniche-Covas, C.; Argüelles-Monal, W.; Román, J. S. *Polym Degrad Stab* 1993, 39, 21.
34. Xiao, B.; Wan, Y.; Zhao, M. Q.; Liu, Y. Q.; Zhang, S. M. *Carbohydr Polym* 2011, 83, 144.
35. Zheng, L. Y.; Zhu, J. F. *Carbohydr Polym* 2003, 54, 527.
36. Qin, C. Q.; Li, H. R.; Xiao, Q.; Liu, Y.; Zhu, J. C.; Du, Y. M. *Carbohydr Polym* 2006, 63, 367.